High-Resolution Lateral Differentiation Using a Macroscopic Probe: XPS of Organic Monolayers on Composite Au−SiO_2 Surfaces

Keren Shabtai,[†] Israel Rubinstein,*[,†] Sidney R. Cohen,[‡] and Hagai Cohen*[,‡]

Contribution from the Department of Materials and Interfaces and Chemical Services Department, Weizmann Institute of Science, Rehovot 76100, Israel

Received October 18, 1999

Abstract: X-ray photoelectron spectroscopy (XPS), an essentially macroscopic probe, is used to analyze mesoscopic systems at a lateral resolution given by the substrate structure. The method is based on controlled differential charging of multi-component surfaces, using a simple, commonly available XPS function, the electron flood gun. This new approach is applied here to a novel composite surface comprising SiO_2 clusters on a {111} gold substrate, onto which different molecules are self-assembled to form a mixed organic monolayer. The method allows direct correlation of adsorbed molecules with surface sites, by analyzing XPS line shifts, which reflect local potential variations resulting from differential surface conductivity. This provides a powerful tool for resolving complex ultrathin films on heterogeneous substrates, on a length scale much smaller than the probe size.

Introduction

The quest to achieve well-defined features which are resolved on the nanometer length scale and distributed in predetermined patterns on solid surfaces is the heart of future optoelectronic devices and a major goal in science and technology. Structural analysis of such systems usually requires scanning probe methodologies, which are essentially small-area techniques. Large-area analytical tools, such as X-ray photoelectron spectroscopy (XPS), are limited in this respect. A fundamental feature of XPS is the contrast between its depth and lateral resolution, typically approaching nm vs μm length scales, respectively. This raises serious problems in the study of nonplanar or heterogeneous surfaces, especially when surface variations fall in the region between the two length scales. For various applications, however, this intermediate region is the relevant one; hence, new high-resolution−large-area characterization methods are crucially needed.

We present here a simple approach where the superior depth resolution of XPS is used to gain lateral sensitivity to surface structural variations that meets the above requirements. It is based on controlled variation of a selected parameter, the excess surface charge, which is sensitive to differences in the local conductivity.

Surface charging in XPS measurements, a consequence of photoelectron emission from insulating samples, is usually considered an experimental obstacle to accurate determination of binding energies.[1−3] It can be compensated for by using an electron flood gun, which stabilizes the energy scale on a reasonably correct value and ensures a nearly homogeneous potential across the studied surface. Yet, differential surface potential, which is harder to eliminate, develops frequently in systems comprised of components with different electrical conductivities.[4−6] Several studies[7−10] have focused on various aspects of charging in XPS, indicating that, on a macroscopic scale, differential surface potential can be analyzed using a classical approach based on charge generation vs discharge rates.[11,12] Application in surface analysis has been demonstrated.[11−16]

With nm-size surface features, more complicated considerations for the charging mechanisms become essential. Factors such as surface conductivity, adhesion quality, geometrical factors, etc., may render this task impossible. Nevertheless, the resultant excess charge, and accordingly, the XPS line shifts, provide a powerful tool for site classification in patterned surfaces. However, with mesoscopic structures the small, naturally occurring positive charging is usually insufficient for satisfactory analysis. We show here that the use of the flood gun at relatively high fluxes, producing *negative* excess charge, leads to larger and well-controlled line shifts required for

* To whom correspondence should be addressed. E-mail: israel.rubinstein@weizmann.ac.il or cphagai@wis.weizmann.ac.il.

[†] Department of Materials and Interfaces.

[‡] Chemical Services Department.

(1) Seah, M. P. In *Practical Surface Analysis*, 2nd ed.; Briggs, D., Seah, M. P., Eds.; Wiley: New York, 1990; Vol. 1, App. 2, p 541 and references therein.

(2) Beamson, G.; Briggs, D. *High-Resolution XPS of Organic Polymers*; Wiley: New York, 1992.

(3) Ogama, T. *J. Vac. Sci. Technol.* **1996**, *A14*, 1309.

(4) Larson, P. E.; Kelly, M. A. *J. Vac. Sci. Technol.* **1998**, *A16*, 3483.

(5) Barr, T. L. In *Practical Surface Analysis*, 2nd ed.; Briggs, D., Seah, M. P., Eds.; Wiley: New York, 1990; Vol. 1, p 357.

(6) Tielsch, B. J.; Fulghum, J. E. *Surf. Interface Anal.* **1996**, *24*, 422.

(7) Lewis, R. T.; Kelley, M. A. *J. Electron Spectrosc. Relat. Phenom.* **1980**, *20*, 105.

(8) Tielsch, B. J.; Fulghum, J. E.; Surman, D. J. *Surf. Interface Anal.* **1996**, *24*, 459.

(9) Tielsch, B. J.; Fulghum, J. E. *Surf. Interface Anal.* **1997**, *25*, 904.

(10) Bandis, C.; Pate, B. B. *Surf. Sci.* **1996**, *345*, L23.

(11) Barr, T. L. *J. Vac. Sci. Technol.* **1989**, *A7*, 1677.

(12) Cazaux, J.; Leheude, P. *J. Electron Spectrosc. Relat. Phenom.* **1992**, *59*, 49.

(13) Miller, J. D.; Harris, W. C.; Zajac, G. W. *Surf. Interface Anal.* **1993**, *20*, 977.

(14) Beamson, G.; Clark, D.; Deegan, D. E.; Hayes, N. W.; Law, D. S−L.; Rasmusson, J. R.; Salaneck, W. R. *Surf. Interface Anal.* **1996**, *24*, 204.

(15) Clark, D. T.; Dilks, A.; Thomas, H. R.; Shuttleworth, D. *J. Polym. Sci. Polym. Chem. Ed.* **1979**, *17*, 627.

(16) Beamson, G.; Bunn, A.; Briggs, D. *Surf. Interface Anal.* **1991**, *17*, 105.

10.1021/ja993710h CCC: $19.00 © 2000 American Chemical Society
Published on Web 05/03/2000

quantitative analysis and site classification. The method is termed controlled surface charging (CSC).

This approach is demonstrated here with a mixed organic monolayer (thiol and silane molecules) self-assembled on a novel composite surface, the latter comprising a conductive substrate (Au) with a non-uniform insulating overlayer (SiO_2). Upon varying the flood-gun electron flux, the dynamic balance of accumulated local surface charge is modified, exhibiting line shifts which can be correlated with the surface structure. As shown below, a qualitative interpretation of line shifts may provide quantitative information on the surface composition and morphology, for example, unequivocally correlating adsorbed molecules with specific surface sites.

Composite Au−SiO_2 surfaces were prepared by controlled diffusion of Si through a gold layer.[17,18] When a gold film (50−100 nm thick) is evaporated onto oxide-free (H-passivated) Si surface and then heated (to ∼100−150 °C) in an oxygen-containing atmosphere, formation of a SiO_2 overlayer on top of the Au film is observed.[19] The process involves diffusion of Si atoms through the Au film to reach the Au/ambient interface, where they are oxidized to form SiO_2 islands (and later, a SiO_2 film).[20] Careful adjustment of the parameters (temperature and duration of heating, Au film thickness, oxygen and moisture content in the contacting gas, Si crystallographic face) provides controlled size and distribution of the insulating islands.[19] The two surface components (Au and SiO_2) differ in both chemical reactivity and electrical conductivity, leading, respectively, to assembly of different molecules at different surface sites, and to the creation of differential charging.

Experimental Section

Substrate Preparation. The studied samples were prepared by resistive evaporation of 50 nm {111}-textured Au onto HF-etched (H-passivated) highly polished doped Si(111) surfaces,[19] followed by annealing in air (24 min at 150 °C, cooled in air to rt).

Monolayer Self-Assembly. The surface was pretreated by UV−ozone + ethanol dip.[21] Decanethiol (DT) was adsorbed (2 h, 4 mM solution in bicyclohexyl), the sample was rinsed with chloroform followed by octadecane trichlorosilane (OTS) adsorption (2 min, 2 mM solution in bicyclohexyl) and rinsing with chloroform.

Scanning Force Microscopy (SFM). SFM measurements were carried out with a Topometrix TMX2010 Discoverer instrument, in the intermittent contact mode.

XPS Measurements. XPS data were collected with an AXIS-HS Kratos instrument, using a monochromatized Al (Kα) source. To eliminate beam-induced damage,[22] a low-source intensity (5 mA, 15 kV) and relatively short scans were used. The spectra shown represent the compromise in signal-to-noise ratio (SNR) required for damage-free data collection. Scanning conditions were determined after systematic study of the damage evolution and its characteristic time scales. Data analysis and conclusions were based on comparison with longer measurements, that is, improved SNR (not shown), performed after the short scans.

The flood-gun flux was controlled via its emission current and two bias voltages. Two extreme cases are considered: "gun-on" (emission current, 1.90 mA; bias, 1.0 and 2.7 V), and "gun-off" (zero e-flux). In the former, a relatively large negative excess charge is supplied to the surface (typical integrated sample current, ∼−300 nA). In the latter, a small positive charge is created, resulting from the photoemission events (typical sample current, ∼1−4 nA). Intermediate flood-gun operating conditions were also tested, showing consistent results (not shown). Data analysis included Shirley background subtraction and Gaussian−Lorenzian line shapes for curve fitting.

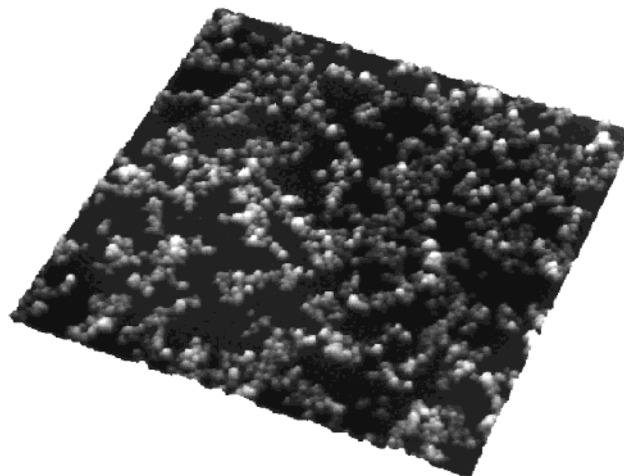

Figure 1. Intermittent contact mode SFM image (5 μm scan; *z*-range, 54 nm) of the composite Au−SiO_2 surface after self-assembly of DT + OTS.

Results and Discussion

Figure 1 shows an SFM image of the composite Au−SiO_2 surface after self-assembly of the mixed monolayer (DT + OTS). The SiO_2 phase appears as grains, 20−30 nm average height and 50−70 nm average diameter,[23] aggregated into larger clusters, randomly distributed on the Au surface.

The XPS spectral response to the flood-gun flux is demonstrated in Figures 2 and 3. The Au (4f) line exhibits no spectral shift, reflecting the good charge compensation across the metallic layer (and the silicon wafer). In contrast, the Si (2s) and O (1s) lines shift by ∼2 eV, attributed to the poor conductivity of the silica grains. This effect forms the basis for the site resolution of the (spectrally similar) adsorbed molecules. Indeed, the C (1s) line splits into several components, subjected to different shifts (Figure 3) which resemble those of the corresponding substrate signals: C_{DT}, exhibiting a negligible shift, is attributed to the molecules adsorbed on gold; C_{OTS}^1 and C_{OTS}^2 are highly shifted components, attributed to the molecules located on different silica sites, as discussed below. Note that the S (2p) line does not shift, confirming its close proximity to the gold substrate, consistent with the adsorption selectivity of the gold for DT molecules. The extracted overall shifts (gun-off vs gun-on peak positions) are given in Table 1.[24]

The gun-off spectral lines are relatively narrow, indicating minor surface potential variations.[25] Yet, accumulation of some excess positive charge on the silica surface is manifested as an asymmetric broadening of the carbon line toward the high binding energy side. In the gun-on spectra, the silica signals reflect grain inhomogeneity. At least two distinct components

(17) Hiraki, A. *Surf. Sci.* **1986**, *168*, 74.
(18) Cros, A.; Dallaporta, H.; Oberlin, J. C. *Appl. Surf. Sci.* **1992**, *56−58*, 434.
(19) Shabtai, K.; Cohen, S. R.; Cohen, H.; Rubinstein, I., in preparation.
(20) When the Au is evaporated on oxide-covered Si, the tendency of Si atoms to diffuse through the Au film is effectively suppressed.
(21) Ron, H.; Matlis, S.; Rubinstein, I. *Langmuir* **1998**, *14*, 1116.
(22) Frydman, E.; Cohen, H.; Maoz, R.; Sagiv, J. *Langmuir* **1997**, *13*, 5089.
(23) The diameter was measured over individual grains after erosion of the tip shape, obtained from the image by blind reconstruction (software developed by A. Efimov, available as freeware at http://www.siliconmdt.com). This procedure gives an upper bound for the true feature size, and yielded diameters 20−40 nm smaller than those measured on the raw image.
(24) Several blank experiments were carried out: (i) The spectral shifts obtained with blank samples (i.e., before monolayer self-assembly) are in good agreement with the results in Table 1. (ii) Electrical isolation of the sample holder almost completely removes the differential effects.
(25) The curve fittings for the gun-off measurements are, therefore, less determining than the gun-on ones.

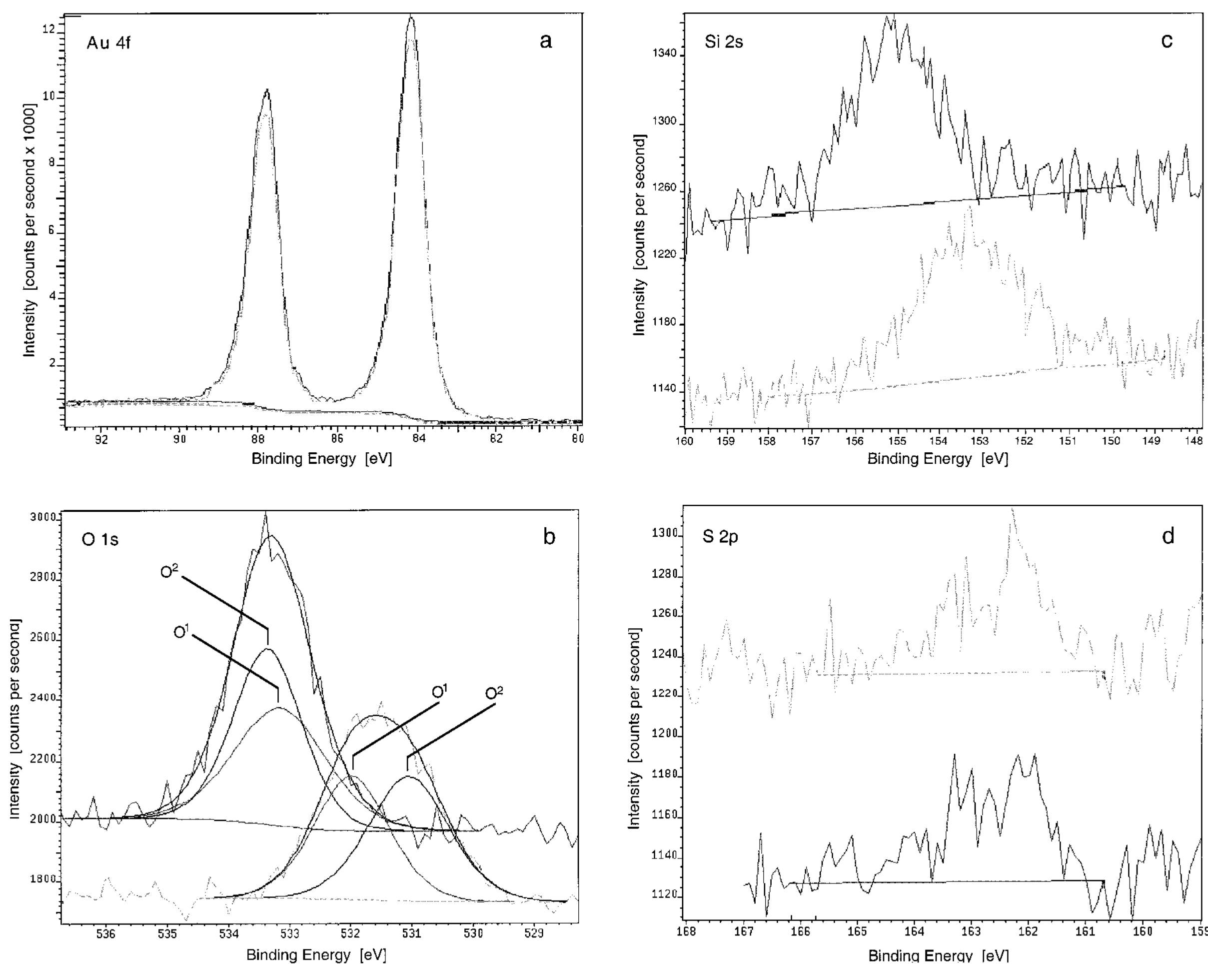

Figure 2. XPS results for the DT + OTS monolayer on the composite Au−SiO_2 surface, showing narrow scans for (a−d) Au, O, Si, and S and line decomposition for O. Top and bottom curves in each plate correspond, respectively, to gun-off and gun-on conditions.

Table 1. Atomic Concentrations and Energy Shifts from XPS Results for the DT + OTS Monolayer on the Composite Au−SiO_2 Surface[a]

	Au	S	Si	O	C	
total conc %	29.4	1.4	8.45	16.1	44.65	
peak shift (eV)	0.0	≤0.05	1.8	1.8	0.7	
	O^1	O^2	C_{DT}	$C_{OTS}{}^1$	$C_{OTS}{}^2$	C_{Im}
line decomposition relative conc %	48.5	51.5	36.8	28.9	30.3	4.1
line decomposition peak shift (eV)	1.25	2.2	0.2	1.2	2.25	2.6

[a] Peak shifts correspond to gun-on vs gun-off measurements (Figures 2 and 3).

within the O line (O^1 and O^2, Figure 2) suggest the existence of two major types of silica grains, subjected to different discharge routes[26] (inclusion of a third component is not justified by the curve fitting; decomposition of the Si line (not shown) is in full agreement with the two-component analysis). This argument is further supported by the C (1s) line decomposition, where the two major shifted components, $C_{OTS}{}^1$ and $C_{OTS}{}^2$, are well correlated with the silica energy shifts, O^1 and O^2 (Table 1).

The results discussed above clearly reveal the site selectivity. However, the power of the CSC method is greatly enhanced by full quantitative analysis of line intensities, where simultaneous agreement of line shifts and intensities would provide a firm confirmation of the qualitative analysis. It should be realized, though, that such an analysis is model-dependent.

The first-order model used here (supported by additional characterization, given elsewhere[19]), assumes rectangular silica grains on a thick gold layer, with average grain height (D) much larger than the relevant electron mean free path (λ). The fraction of gold surface covered with silica is denoted θ. DT molecules are assumed to bind selectively to the gold at a relative coverage θ_{DT}, with a layer thickness 1.8 times shorter than that of the OTS fraction, the latter being selectively bound to the silica at a relative coverage θ_{OTS}. Extraction of the coverage parameters was carried out by fitting the theoretical expressions to the experimental element concentrations (before line decomposition).[27] The values obtained are: $\theta = 0.53$; $\theta_{DT} = 1.00$; $\theta_{OTS} = 0.95$ (estimated relative errors, <5%), consistent with the expected site selectivity and suggesting nearly full coverage by the thiol and the silane. These results fully agree with the independently derived values of C_{DT}: C_{OTS} and C_{DT}: S[28] (the latter verified by much longer scans), obtained from line

(26) The existence of "second layer" grains has been suggested by SFM measurements. The relative abundance of the two components depends on the sample preparation details, and will be discussed elsewhere.[19]

(27) Details on the data analysis and models used are given as Supporting Information.

(28) For accurate determination of the theoretical ratio C_{DT}: S, we used a discrete summation over the thiol C atoms, yielding

$$\sum_{n=0}^{9}[\exp(-n\delta/\lambda)] = [1 - \exp(-9\delta/\lambda)]/[1 - \exp(-\delta/\lambda)]$$

where δ is the projection of the interatomic (C−C) distance along the vertical axis.

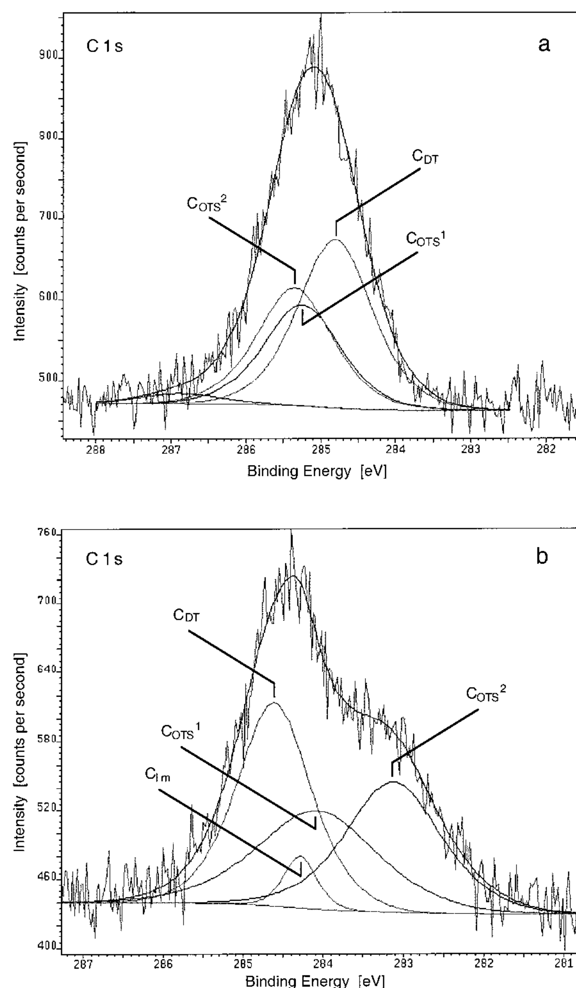

Figure 3. XPS results for the DT + OTS monolayer on the composite Au−SiO_2 surface, showing narrow scans and line decomposition for C. (a) and (b) represent, respectively, gun-off and gun-on conditions.

decomposition. The value of θ is in good agreement with independent measurements of the silica coverage.[19]

The calculation was repeated with different model structures for the grains, for example, grains with inclined side-faces.[27] The calculated parameters converge within ±7%, exhibiting limited sensitivity to the chosen model structure.[29] The estimated overall accuracy of the analysis is better than ±10%. Note that accuracy is expected to improve substantially when applied to ordered (patterned) substrates, where the complexity of solving the substrate and overlayer parameters simultaneously can be eliminated.

Conclusions

In conclusion, a powerful application of XPS is presented, based on the information provided by discharge processes. The method is simple and exceedingly useful for analyzing complex systems, such as patterned surfaces presenting large variations in the local electrical conductivity. Controlled manipulation of a common XPS accessory, the flood gun, allows accurate site classification, translated to nanometer-scale lateral differentiation of multi-component overlayers. This approach is shown to provide quantitative analysis of disordered micro- or meso-scale features on composite macroscopic areas. In the present work the method was applied to a novel Au−SiO_2 surface, demonstrating molecular differentiation in a mixed monolayer on a composite surface. Application to well-defined (e.g., lithographic) heterostructures would simplify the analysis and improve its accuracy considerably, such that a true lateral resolution may be achieved. With certain modification, the CSC technique can also be used for high-resolution depth profiling.[30]

Acknowledgment. I. Rubinstein acknowledges support of this work by the U.S.−Israel Binational Science Foundation and the Klutznick Fund (Weizmann Institute). Helpful discussions with A. Vaskevich are gratefully acknowledged.

Supporting Information Available: Schemes 1 and 2 and relevant calculations (PDF). This material is available free of charge via the Internet at http://pubs.acs.org.

JA993710H

(29) The 4% C_{Im} signal at 284.3 eV (gun-on, Figure 3b), small within the present accuracy limitations, appears to originate from silica sites, and is attributed to a small amount of oxidized carbon contamination on the strongly shifted silica component. The weak signal observed around 286.9 eV in the gun-off spectrum (Figure 3a) could arise from the same contamination. (The possibility that C_{Im} is related to grain edges, namely, to silica regions relatively close to the gold, is ruled out due to lack of a corresponding feature in the O line shape).

(30) Doron-Mor, I.; Hatzor, A.; Vaskevich, A.; Shanzer, A.; Rubinstein, I.; Cohen, H., manuscript submitted.